(24) Y.-H. Chen, J. T. Yang, and H. M. Martinez, *Biochemistry*, **11**, 4120 (1972).
(25) K. Itoh and T. Shimanouchi, *Biopolymers*, **9**, 383 (1970).
(26) F. H. C. Crick and A. Rich, *Nature (London)*, **176**, 780 (1955).
(27) A. W. McLellan and G. A. Melson, *J. Chem. Soc. A*, 137 (1967).
(28) L. Simons, G. Bertstrom, G. Blomfelt, S. Forss, H. Stenback, and G. Wansen, *Comments Phys. Math., Soc. Sci, Fenn., Helsinki-Helsingfors*, **42**, 125 (1972).
(29) F. Heitz, B. Lotz, and G. Spach, *J. Mol. Biol.*, **92**, 1 (1975).

Structural and Electronic Spectroscopic Investigation of $[(Me_2N)_3C_3]_2[Pt_2Cl_6]$

Charles D. Cowman, Jack C. Thibeault, Ronald F. Ziolo, and Harry B. Gray*

Contribution No. 5097 from the Arthur Amos Noyes Laboratory of Chemical Physics, California Institute of Technology, Pasadena, California 91125.
Received April 25, 1975

Abstract: The crystal structure of $[(Me_2N)_3C_3]_2[Pt_2Cl_6]$ has been determined from three-dimensional x-ray data collected by counter techniques using Mo Kα monochromatized radiation. The structure was refined by full-matrix least-squares methods using 4451 nonzero reflections for which $F^2 > \sigma(F^2)$, and assuming anisotropic thermal motion for all nonhydrogen atoms. The least-squares refinement led to a final value of the conventional R factor (on F) of 0.058. Crystal data are as follows: monoclinic, space group $P2_1/c$; a = 17.383 (11), b = 11.234 (6), c = 17.192 (11) Å; β = 117.46 (5)° (23 °C); Z = 4; d_{obsd} = 2.12, d_{calcd} = 2.09 g/cm^3. Discrete $Pt_2Cl_6^{2-}$ anions are sandwiched between two parallel cyclopropenium cations. These sandwiched units are in turn stacked to form zigzag chains parallel to the crystallographic b axis. The two crystallographically independent cyclopropenium cations do not differ significantly. Coordination about each platinum atom in $Pt_2Cl_6^{2-}$ is planar to a good approximation, but there is a fold of 10 (1)° about the Cl(1)-Cl(2) axis. The Pt-Pt distance in the anion is 3.481 (2) Å. The polarized electronic absorption spectra of a single crystal of $[(Me_2N)_3C_3]_2[Pt_2Cl_6]$ have been measured at 5 K. The spectra have been resolved into absorption profiles along the molecular axes of $Pt_2Cl_6^{2-}$. Three prominent y-polarized bands are observed, at 19 650, 24 600, and 26 250 cm^{-1}. The 19 650-cm^{-1} band is assigned to the y-allowed transition $^1A_g \rightarrow B_{2u}$ (^3A_u), whereas the 24 600- and 26 250-cm^{-1} features are attributed to $^1A_g \rightarrow B_{2u}$ ($^1B_{2u}$) excitations derived from $^1A_{1g} \rightarrow {}^1A_{2g}$ ($d_{x^2-y^2} \rightarrow d_{xy}$) in D_{4h} $PtCl_4^{2-}$. The intensity enhancement of the $^1A_g \rightarrow B_{2u}$ (^3A_u) transition and the 1650-cm^{-1} splitting observed for the $^1A_g \rightarrow B_{2u}$ ($^1B_{2u}$) bands conclusively establish that moderate Pt···Pt interactions are present in $Pt_2Cl_6^{2-}$. Detailed examination of the $Pt_2Cl_6^{2-}$ polarized spectra also shows that the lowest excited states in the $[Pt^{II}Cl_4]$ chromophore increase energetically according to $^3E_g < {}^3A_{2g} < {}^3B_{1g} < {}^1A_{2g}$.

There has been considerable recent interest in the electronic spectra of Pt(II) complexes in which direct metal-metal interactions are present.[1] Perhaps the best studied cases are the double salts, such as $[Pt(NH_3)_4][PtCl_4]$ (Magnus' green salt), in which the planar units stack face-to-face in infinite columns.[1] Much less is known, however, about the extent of Pt···Pt interaction in planar, dihalobridged complexes of the type $Pt_2X_6^{2-}$. The polarized electronic absorption spectra of a single crystal of $[Et_4N]_2[Pt_2Br_6]$ were interpreted by Day et al.[2] in terms of an effectively isolated $[Pt^{II}Br_4]$ chromophore, although later work by Martin[3] on the same system has indicated that some Pt···Pt interaction is present.

We have chosen to probe the $Pt_2Cl_6^{2-}$ complex for possible Pt···Pt interactions, as the electronic structure of the reference monomer, $PtCl_4^{2-}$, has been exhaustively investigated by theoretical and experimental methods.[4] Here we report full details of the x-ray structure analysis[5] and the 5 K polarized electronic absorption spectra of a single crystal of $[(Me_2N)_3C_3]_2[Pt_2Cl_6]$.

Experimental Section

Collection and Reduction of X-Ray Intensity Data. A well-formed crystal of $[(Me_2N)_3C_3]_2[Pt_2Cl_6]$,[6] shaped like an octahedron compressed along the C_3 axis, was chosen for x-ray diffraction study. The crystal had eight well-developed faces and gave good optical extinction between crossed polarizers. It was mounted with the b axis (from extinction direction and dichroism) approximately parallel to the rotation axis. A series of Weissenberg and precession photographs taken with Mo Kα and Cu Kα radiations indicated systematic absences of reflections $h0l$ with l odd and $0k0$ with k odd. The crystals were assigned to the monoclinic system, space group $P2_1/c$. The measured density of the crystal, by CCl_4 displacement, is 2.12 g/cm^3. The calculated density, assuming four formula units per unit cell, is 2.09 g/cm^3.

Fourteen reflections ($2\theta > 20°$) were centered in the counter aperture by varying 2θ, ϕ, and χ in conjunction with the left-right and top-bottom balancing features of the variable receiving aperture. The cell constants and their standard deviations were determined by a least-squares refinement of the 2θ values for these 14 reflections. The results (Mo K$\bar{\alpha}$ radiation, λ 0.71069) are a = 17.383 (11) Å, b = 11.234 (6) Å, c = 17.192 (11) Å, and β = 117.46 (5)° (23 °C). The corresponding ϕ and χ values for 13 of the reflections were used as input data for the orientation program operating under the CRYM crystallographic computing system.[7] The independent intensity data set was collected at 23 °C from a single-crystal mounted with its b axis approximately parallel to the ϕ axis of a Datex-automated General Electric diffractometer.

A total of 5248 independent reflections were collected by the θ-2θ scan technique in the range $4° < 2\theta$ (Mo K$\bar{\alpha}$) $\leq 50°$. A takeoff angle of 3° was used with the counter wide open. A check of several high-angle reflections indicated that our settings included the entire peak in the scan. The pulse height analyzer was set for approximately a 90% window centered on the Mo Kα peak. Mo K$\bar{\alpha}$ monochromatized radiation, obtained by using a single graphite crystal, was used for data collection. A scan rate of 1°/min (in 2θ) was used with stationary counter, stationary crystal background counts of 30 s duration taken at each end of the scan. A symmetric scan range of between 1.5 and 2.0° was adjusted to account for α_1-α_2 splitting.

Throughout the data collection the intensities of three reference reflections were measured every 60 reflections. There were no signs of crystal decomposition in the x-ray beam.

The values for the observed intensities, I_{obsd}, were derived from the scalar counts using the formula

$$I_{obsd} = S - \frac{B_1 + B_2}{2}\left(\frac{t}{30}\right)$$

Table I. Positional and Thermal Parameters of the Heavy Atoms[a,b]

Atom	x	y	z	β_{11}	β_{22}	β_{33}	β_{12}	β_{13}	β_{23}
Pt1	1668 (0.2)	486 (0.4)	2892 (0.3)	38 (0.2)	80 (0.4)	57 (0.3)	−3 (0.5)	51 (0.4)	6 (0.6)
Pt2	3419 (0.2)	9453 (0.4)	2692 (0.2)	40 (0.2)	80 (0.4)	47 (0.2)	−13 (0.5)	48 (0.4)	0 (0.5)
Cl1	3103 (2)	9990 (3)	3824 (2)	41 (1)	155 (3)	52 (1)	6 (4)	50 (2)	−1 (4)
Cl2	2052 (2)	195 (3)	1770 (2)	46 (1)	181 (4)	53 (2)	10 (4)	47 (2)	33 (4)
Cl3	1386 (2)	702 (3)	4054 (2)	60 (2)	167 (4)	74 (2)	20 (4)	84 (3)	−30 (4)
Cl4	287 (2)	948 (3)	1910 (2)	43 (2)	158 (4)	89 (2)	35 (4)	51 (3)	67 (5)
Cl5	3642 (2)	8972 (3)	1524 (2)	77 (2)	141 (3)	60 (2)	−1 (4)	88 (3)	−25 (4)
Cl6	4750 (2)	8791 (3)	3662 (2)	50 (2)	134 (3)	72 (2)	30 (4)	60 (3)	41 (4)
C1	2215 (6)	3525 (8)	2731 (6)	50 (6)	62 (9)	35 (5)	−8 (12)	42 (9)	2 (11)
C2	3049 (6)	3176 (8)	3166 (5)	46 (5)	85 (10)	30 (4)	3 (12)	37 (8)	−11 (11)
C3	2606 (6)	3451 (9)	3644 (6)	46 (6)	83 (6)	51 (6)	−5 (13)	54 (10)	−3 (10)
C4	1470 (8)	3549 (12)	1177 (6)	70 (7)	162 (16)	38 (6)	5 (19)	32 (10)	−14 (16)
C5	3794 (8)	2645 (10)	2340 (7)	72 (7)	130 (14)	69 (7)	−27 (18)	92 (12)	−54 (16)
C6	4536 (7)	2456 (13)	3963 (8)	37 (6)	238 (20)	73 (7)	11 (18)	19 (11)	−106 (21)
C7	3288 (9)	3129 (13)	5181 (6)	114 (10)	224 (20)	26 (5)	3 (24)	59 (12)	54 (18)
C8	1819 (9)	3919 (12)	4453 (9)	119 (10)	180 (17)	107 (10)	−73 (22)	183 (18)	−142 (21)
C9	720 (8)	4133 (11)	2024 (8)	61 (7)	140 (16)	76 (8)	18 (17)	37 (12)	−4 (17)
C10	7507 (7)	1605 (8)	2323 (6)	67 (6)	85 (10)	33 (5)	47 (13)	62 (10)	13 (12)
C11	8028 (7)	1745 (9)	3211 (7)	46 (6)	87 (11)	61 (6)	10 (14)	59 (11)	15 (14)
C12	7222 (6)	1318 (9)	2925 (6)	41 (5)	88 (11)	41 (5)	30 (13)	30 (9)	18 (12)
C13	6536 (9)	1465 (12)	789 (7)	114 (10)	168 (16)	42 (6)	104 (22)	64 (13)	3 (17)
C14	8052 (9)	2127 (11)	1318 (7)	112 (10)	139 (15)	67 (7)	70 (20)	132 (15)	38 (17)
C15	9459 (8)	2631 (13)	3695 (9)	54 (7)	177 (18)	116 (10)	−2 (19)	88 (14)	19 (22)
C16	8839 (8)	2267 (14)	4732 (7)	66 (7)	262 (23)	59 (7)	−17 (22)	39 (11)	−102 (21)
C17	6694 (8)	884 (11)	3967 (8)	75 (8)	169 (16)	70 (7)	−12 (18)	100 (13)	53 (17)
C18	5724 (7)	740 (11)	2372 (8)	42 (6)	162 (17)	92 (8)	−8 (17)	53 (12)	100 (19)
N1	1520 (5)	3804 (8)	2017 (5)	44 (5)	124 (10)	46 (4)	6 (12)	30 (8)	−38 (11)
N2	3772 (5)	2815 (8)	3172 (5)	49 (5)	113 (10)	49 (5)	−9 (12)	57 (8)	6 (11)
N3	2609 (6)	3589 (8)	4400 (6)	79 (6)	123 (11)	53 (5)	1 (14)	77 (10)	15 (13)
N4	7397 (6)	1623 (9)	1507 (6)	58 (6)	156 (12)	58 (5)	55 (14)	56 (9)	7 (14)
N5	8771 (6)	2093 (8)	3858 (6)	46 (5)	127 (10)	57 (5)	−1 (12)	49 (8)	1 (12)
N6	6594 (5)	880 (7)	3073 (5)	41 (4)	120 (10)	58 (5)	−1 (11)	56 (8)	−23 (11)

[a] The atom labeling scheme is given in Figures 2 and 3 and in footnote *b* of Table III. Positional and thermal parameters have been multiplied by 10^4. The estimated standard deviations in the least significant figure(s) as derived from the inverse matrix of the final least-squares refinement cycle are given in parentheses in this and subsequent tables. [b] The temperature factors are of the form $\exp[-(\beta_{11}h^2 + \beta_{22}k^2 + \beta_{33}l^2 + \beta_{12}hk + \beta_{13}hl + \beta_{23}kl)]$.

where S is the scan count, B_1 and B_2 are the two background counts, and t is the scan time in seconds. Negative values of I_{obsd} calculated from this formula were set equal to zero. The standard deviation for each reflection was calculated using

$$\sigma^2(I_{obsd}) = S + \frac{B_1 + B_2}{2}\left(\frac{t}{30}\right)^2 + (0.02S)^2$$

The last term in this equation is an empirical term (Busing and Levy)[8] which presumably allows for errors not due to counting statistics. The standard deviations calculated in this way were the basis for the weights used in the least-squares refinement. The intensities and their standard deviations were corrected for Lorentz and polarization effects and for absorption using the numerical Gaussian quadrature method.[9] The linear absorption coefficient (Mo K$\bar{\alpha}$) for this compound is 104.1 cm^{-1}, and the transmission coefficients for the selected crystal range from 0.3360 for the $\bar{1}13$ reflection to 0.1515 for the 120 reflection. The multifaceted crystal used in the x-ray characterization was characterized by bounding planes (100), ($\bar{1}00$), (001), (00$\bar{1}$), (1$\bar{1}\bar{1}$), ($\bar{1}$11), ($\bar{1}\bar{1}$1), and (11$\bar{1}$), and appropriate dimensional measurements. The longest distance from point to point through the crystal measured 1.34 mm. The data were put on an approximately absolute scale with a Wilson plot.[10] The distribution of the normalized structure factors[11] and application of the zero moment test of Howells, Phillips, and Rogers[12] suggested a centric space group in accord with our assignment $P2_1/c$. Of the 5248 reflections collected, 4451 obeyed the condition $F^2 > \sigma(F^2)$ and were used in subsequent calculations.

Elucidation and Refinement of the Structure. Heavy-atom methods were applied to solve the structure. The positions of the two platinum atoms were readily determined from a three-dimensional Patterson function calculation. Structure factors calculated on the basis of the coordinates of these atoms led to an R index ($R = \Sigma||F_o| - |F_c||/\Sigma|F_o|$) of 0.512. A subsequent Fourier map was used to locate the six chlorine atoms. Three cycles of full-matrix least-squares refinement of the coordinates and isotropic temperature factors of these eight atoms reduced the R index to 0.174. Only one subsequent Fourier map was needed to locate all of the carbon and nitrogen atoms. Introduction of anisotropic temperature factors for all these atoms at this point further reduced the R index to 0.064. The hydrogen atom positions were located on a difference Fourier map in conjunction with calculations based upon tetrahedral geometry for the methyl carbon atoms assuming a C–H distance of 0.90 Å and that (1) the three generated H atoms describe a plane normal to the N–CH_3 bond, (2) the three angles at the methyl C atom between N and each generated H atom are greater than 90°, and (3) atom C′ of the C′H_3–N–CH_3 unit is staggered with respect to the generated atoms in a projection down the N–CH_3 bond. Each hydrogen atom was assigned an isotropic temperature factor one unit higher than the value of the last refined such factor for the atom attached to it. Inclusion of the hydrogen parameters in a structure factor calculation reduced the R index by 0.002.

A comparison of the F_o and F_c values for several low angle reflections, particularly the 002 and 200, suggested the presence of a secondary extinction effect and in the final least-squares cycles 326 parameters were adjusted; these included a scale factor, a secondary extinction factor,[13a] and the positional parameters of all of the 32 heavy atoms and their anisotropic temperature factors. The 326 parameters were apportioned between two complete matrices. Hydrogen positional and thermal parameters were not included in the refinement.

All calculations were carried out on an IBM 370/155 computer using subprograms operating under the CRYM system.[7] The quantity $\Sigma w(F_o^2 - F_c^{*2})^2$, where $w = 1/\sigma^2(F_o^2)$ and F_c^* is as defined by Larson's equation 3,[13b] was minimized throughout the least-squares refinement. Atomic form factors for Pt, Cl, C, and N were taken from Hanson, Herman, Lea, and Skillman,[14] the value for Pt being reduced by 2.05 electrons to take account of the real part of anomalous dis-

Table II. Positional and Thermal Parameters of the Hydrogen Atoms[a-c]

Atom	x	y	z	B
H1(C4)	199	330	122	5.8
H2	127	417	80	
H3	110	291	91	
H4(C5)	330	293	187	5.5
H5	388	189	223	
H6	425	308	232	
H7(C6)	445	258	445	6.7
H8	502	286	405	
H9	464	166	396	
H10(C7)	377	296	511	6.7
H11	314	245	537	
H12	347	366	564	
H13(C8)	150	366	394	6.7
H14	192	445	487	
H15	160	324	460	
H16(C9)	78	428	257	6.9
H17	30	354	180	
H18	47	480	170	
H19(C13)	649	115	98	6.3
H20	652	97	36	
H21	629	217	523	
H22(C14)	857	216	182	5.9
H23	792	286	109	
H24	815	166	93	
H25(C15)	938	250	314	7.1
H26	1000	236	406	
H27	949	346	376	
H28(C16)	840	191	479	6.7
H29	883	306	486	
H30	935	196	516	
H31(C17)	728	975	439	6.2
H32	652	19	412	
H33	641	149	408	
H34(C18)	572	76	184	6.1
H35	537	134	237	
H36	549	4	241	

[a] The positional parameters have been multiplied by 10^3. [b] Hydrogen atoms are bonded to the atom given in parentheses. No designation indicates bonding to the atom in parentheses immediately above the hydrogen. [c] Hydrogen atoms were assigned an isotropic temperature factor one unit higher than the value of the last refined isotropic temperature factor for the atom to which the hydrogen is attached.

persion.[15] $\Delta f''$ was ignored. The atomic form factor for hydrogen used was that calculated by Stewart, Davidson, and Simpson.[16]

In the final cycle of refinement no heavy-atom parameter shifted by as much as 0.5 esd. The final R index for 4451 reflections above σ is 0.058 and the goodness of fit, $[\Sigma w(F_o^2 - F_c^2)^2/(m-s)]^{1/2}$, where m is the number of reflections and s the number of refinable parameters, is 1.70. The final value of the secondary extinction parameter, g, as defined by Larson's equation 3,[13b] is $(0.83 \pm 0.05) \times 10^{-7}$. Inclusion of the secondary extinction correction in the refinement reduced R by 0.004 with the final value for R' ($R' = \Sigma w^2(F_o^2 - F_c^2)^2/\Sigma w^2 F_o^4$) being 0.007. On a final difference Fourier synthesis the highest peak was 0.3 $e^-/Å$, as compared with the value 0.5 $e^-/Å$ for a typical hydrogen atom in this structure. The final parameters and their estimated standard deviations for the heavy atoms and for the hydrogen atoms are given in Tables I and II, respectively. The estimated standard deviations in the positions of the platinum and chlorine atoms are approximately 0.0005 Å, whereas those for the carbon and nitrogen atoms are about 0.013 Å. The values of the observed and calculated structure factors (in electrons × 10) are available.[17]

Electronic Absorption Spectral Measurements. Large single crystals of $[(Me_2N)_3C_3]_2[Pt_2Cl_6]$, which had been grown from acetone, were generously provided by D. C. Harris. The crystals were imbedded in paraffin and solvent ground using acetonitrile–hexane. The diamond-shaped (100) face appears red along c and pink along the b axis; the square (111) face is also dichroic, pink to yellow. Crystals were mounted with epoxy over pinholes cut in lead foil. Single-crystal polarized spectra were measured on a Cary 17 spectrophotometer equipped with an Andonian Associates liquid helium Dewar and double Glan-Taylor air-spaced calcite polarizers by procedures that have been described in detail elsewhere.[18]

Spectra were measured along the extinction directions of the crystals: (100) $\parallel = \bar{b}$, $\perp = \bar{c}$, $A_\parallel = 0.8836A_z + 0.1115A_x + 0.0055A_y$, $A_\perp = 0.0131A_z + 0.2617A_x + 0.7247A_y$; (111) $\parallel = -0.5321\bar{a}^* + 0.7913\bar{b} - 0.3254\bar{c}$, $\perp = -0.5217\bar{a}^* + 0.8530\bar{c}$, $\bar{A}_\parallel = 0.6144A_z + 0.1330A_x + 0.2527A_y$, $\bar{A}_\perp = 0.0708A_z + 0.7215A_x + 0.2077A_y$.

Results and Discussion

A stereoscopic view of the unit cell contents is shown in Figure 1. Discrete $Pt_2Cl_6^{2-}$ anions are sandwiched between two approximately parallel $(Me_2N)_3C_3^+$ groups with an interionic approach distance of slightly less than 4 Å. The cyclopropenium cations are staggered such that each is in the vicinity of a different Pt atom. The $(Me_2N)_3C_3^+$ ions in adjacent sandwiched units are stacked back to back, with an approximately 4 Å separation, thereby forming zigzag chains parallel to the b axis. The interatomic distances and angles for $Pt_2Cl_6^{2-}$ and the two crystallographically independent cations are given in Table III.

The dichloro-bridged $Pt_2Cl_6^{2-}$ anion deviates slightly from planarity, owing to a bend or fold of the Pt_2Cl_2 ring along the line joining the bridging chlorine atoms (Figure 2). The dihedral angle subtended by the two planes formed from the bridging chlorine atoms and one platinum atom from each half of the anion is only slightly displaced from its respective three-atom plane; there are significant deviations, as would be expected, from the least-squares plane through the entire anion, with the bridging chlorine atoms on one side of the plane and the four terminal chlorine atoms on the other side (Table V). The fold or bend in the anion, away from cation I and toward cation II, appears to be a consequence of the overall

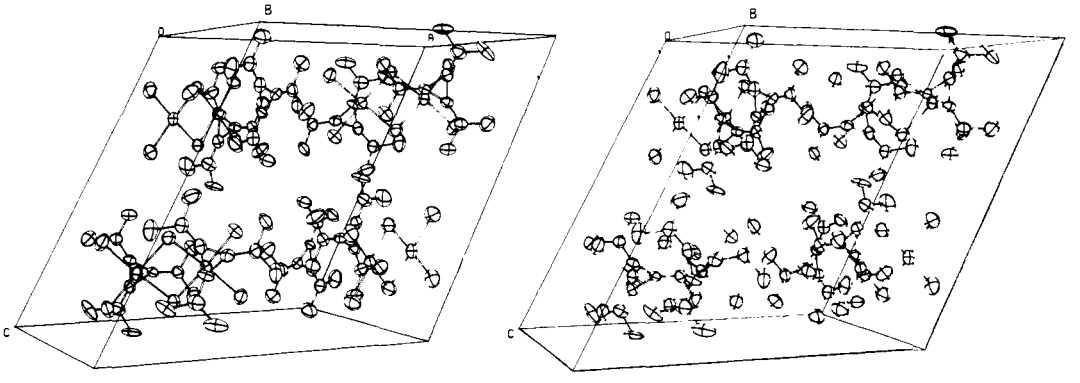

Figure 1. A stereoscopic view of the packing in a unit cell of $[(Me_2N)_3C_3]_2[Pt_2Cl_6]$. Hydrogen atoms have been omitted.

Table III. Interatomic Distances (Å) and Angles (deg)[a]

Atoms	Angles	Atoms	Angles
	Anion		
Pt1-Cl1-Pt2	94.4 (1)	N1-C1-C2	152.4 (12)
Pt1-Cl2-Pt2	94.5 (1)	C1-C2-N2	150.9 (10)
Cl1-Pt1-Cl2	84.9 (1)	N2-C2-C3	148.0 (8)
Cl1-Pt2-Cl2	85.2 (1)	C2-C3-N3	149.5 (8)
Cl1-Pt1-Cl3	91.0 (1)	N3-C3-C1	152.6 (11)
Cl2-Pt1-Cl4	91.4 (1)	C3-C1-N1	146.4 (12)
Cl3-Pt1-Cl4	92.6 (1)	C1-N1-C9	122.1 (10)
Cl5-Pt2-Cl6	92.2 (1)	C9-N1-C4	116.6 (8)
Cl5-Pt2-Cl2	91.1 (1)	C1-N1-C4	120.0 (10)
Cl6-Pt2-Cl1	91.4 (1)	C2-N2-C5	119.2 (8)
		C5-N2-C6	117.2 (10)
		C2-N2-C6	123.3 (10)
	Cation I		
C3-C1-C2	61.1 (7)	C3-N3-C7	121.3 (11)
C1-C2-C3	61.1 (8)	C7-N3-C8	115.4 (11)
C2-C3-C1	57.7 (7)	C3-N3-C8	121.2 (8)
	Cation II		
Atoms 1-2-3[b]	Angles	Atoms	Distances
C12-C10-C11	58.3 (8)	1-2	1.376 (17)
C10-C11-C12	60.8 (8)	1-2	1.378 (13)
C11-C12-C10	60.9 (8)	1-2	1.342 (15)
N4-C10-C11	150.4 (12)	1-2	1.327 (15)
C10-C11-N5	149.0 (14)		
N5-C11-C12	150.1 (13)	1-2	1.317 (12)
C11-C12-N6	151.3 (10)		
N6-C12-C10	147.8 (8)	1-2	1.324 (16)
C12-C10-N4	150.8 (9)		
C10-N4-C13	119.3 (12)	2-3	1.446 (14)
C13-N4-C14	118.1 (10)	2-3	1.436 (20)
C10-N4-C14	120.2 (8)		
C11-N5-C15	121.7 (11)	2-3	1.478 (19)
C15-N5-C16	116.8 (9)	2-3	1.465 (17)
C11-N5-C16	119.3 (11)		
C12-N6-C17	119.3 (8)	2-3	1.463 (17)
C17-N6-C18	116.7 (11)	2-3	1.442 (12)
C12-N6-C18	121.2 (10)		

[a] Distances for the anion and cation I are given in Figures 2 and 3, respectively. [b] The atom numbering scheme for cation II, in the format C_{ring}-N(CH_3,CH_3), is 10-4(13, 14), 11-5(15, 16), and 12-6(17, 18).

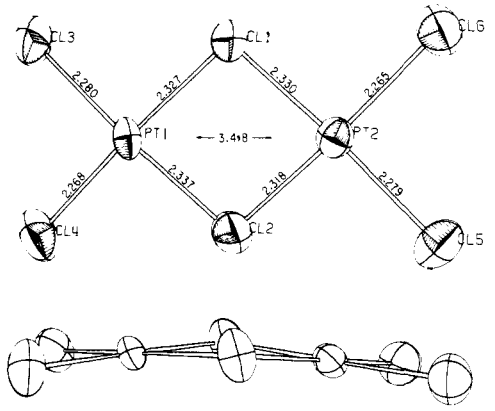

Figure 2. Thermal ellipsoids (40% probability) and interatomic distances for $Pt_2Cl_6^{2-}$.

nature of the packing. Aside from the normal interionic approach distances on the order of 3.7–3.8 Å, we note three short cation–anion contacts: Pt1-C1, 3.589 (8) Å; Pt2-C10 ($1 - x$, $\frac{1}{2} + y$, $\frac{1}{2} - z$), 3.576 (7) Å; and C14-C9, 3.643 (10) Å.

The Pt-Pt distance of 3.418 (1) Å is shorter, as expected, than that in the structurally similar $Pt_2Br_6^{2-}$ ion (3.55 (2) Å).[19] The platinum–chlorine distances are in reasonable agreement with the sum of the respective single-bond covalent radii. The endocyclic distances are slightly greater than the exocyclic ones ($\Delta \sim 0.06$ Å), as has also been observed in the $Cu_2Cl_6^{2-}$ ion ($\Delta \sim 0.04$ Å)[19] and in Al_2Cl_6 and Al_2Br_6.[20]

The X-Pt-X angles in the four-membered Pt_2X_2 ring deviate significantly from 90° in both $Pt_2Cl_6^{2-}$ and $Pt_2Br_6^{2-}$.[19] Stephenson explained this distortion in $Pt_2Br_6^{2-}$ in terms of the differing repulsions between pairs of bromide ions.[19] Owing to their higher coordination, the bridging ligands (Br1 and Br_2, using a numbering system analogous to that in Figure 2) should have a slightly smaller negative charge than the terminal ones (Br3 and Br4). The repulsive force between Br3 and Br4 is therefore expected to be greater than that between Br3 and Br1, which in turn is expected to be greater than that between Br1 and Br2. The angles found in $Pt_2Br_6^{2-}$ (Br3-Pt1-Br4 = 93.78°, Br3-Pt1-Br1 = 89.94°, and Br1-Pt1-Br2 = 86.19°) are in good agreement with this prediction. The differences between successive angles are both approximately 4°. A similar effect appears to operate in $Pt_2Cl_6^{2-}$, as the Cl1-Pt1-Cl2 angle is 84.9°.

Table IV. Planes through Three-Atom Rings[a]

Anion		Cation I		Cation II	
Atom	Dev, Å	Atom	Dev, Å	Atom	Dev, Å
Pt1*	0.0	C1*	0.0	C10*	0.0
Cl1*	0.0	C2*	0.0	C11*	0.0
Cl2*	0.0	C3*	0.0	C12*	0.0
Cl3	−0.040	N1	−0.034	N4	+0.078
Cl4	−0.005	N2	+0.013	N5	−0.029
		N3	−0.048	N6	+0.036
		C4	+0.152	C13	−0.151
Pt2*	0.0	C5	+0.071	C14	−0.002
Cl1*	0.0	C6	+0.108	C15	−0.128
Cl2*	0.0	C7	+0.197	C16	−0.345
Cl5	+0.002	C8	+0.015	C17	−0.086
Cl6	−0.041	C9	+0.029	C18	−0.220

Planes

Anion Pt1: $+0.385X + 0.917Y - 0.106Z - 0.078 = 0$
Anion Pt2: $-0.574X - 0.790Y + 0.215Z + 0.095 = 0$
Cation I: $-0.433X - 0.894Y + 0.112Z + 0.380 = 0$
Cation II: $+0.506X - 0.847Y - 0.163Z - 0.206 = 0$

Dihedral Angle

Interplanar Pt1Cl1Cl2, Pt2Cl1Cl2 angle: 170.0°

[a] Planes are defined in the real monoclinic coordinates X, Y, Z, and are calculated using unit weight for atoms marked with an asterisk.

Table V. Least-Squares Planes in $[(Me_2N)_3C_3]_2[Pt_2Cl_6]$[a]

Anion		Cation I		Cation II	
Atom	Dev, Å	Atom	Dev, Å	Atom	Dev, Å
Pt1	+0.041	C1	−0.015	C10	+0.030
Pt2	+0.022	C2	0.000	C11	−0.005
Cl1	+0.179	C3	−0.020	C12	+0.016
Cl2	+0.182	N1	+0.013	N4	−0.020
Cl3	−0.127	N2	+0.007	N5	−0.007
Cl4	−0.090	N3	+0.015	N6	−0.015
Cl5	−0.123				
Cl6	−0.084				

Planes

Anion: $0.339X + 0.940Y + 0.047Z - 0.883 = 0$
Cation I: $0.312X + 0.948Y + 0.063Z - 4.558 = 0$
Cation II: $-0.367X + 0.927Y - 0.079Z + 2.754 = 0$

[a] Planes are defined in the orthogonalized coordinates X, Y, Z, and are calculated using unit weight for all atoms.

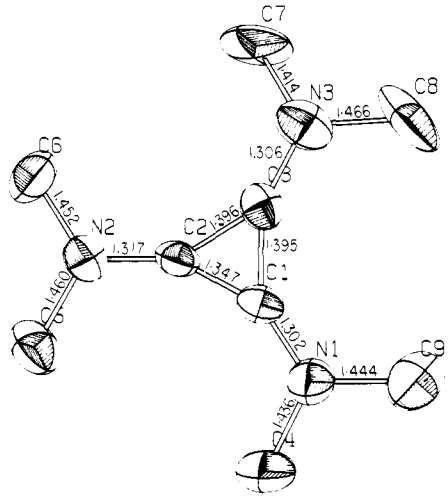

Figure 3. Thermal ellipsoids (40% probability) and interatomic distances for $(Me_2N)_3C_3^+$ (I).

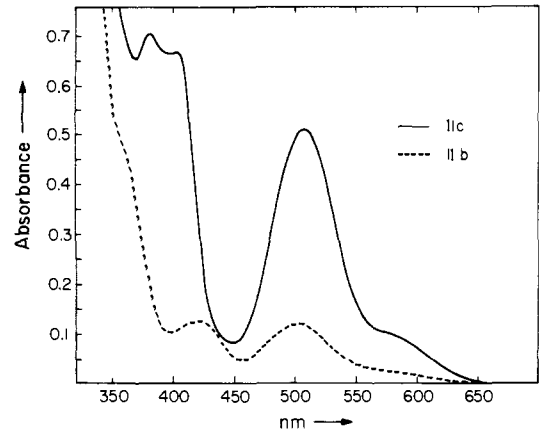

Figure 4. Polarized crystal absorption spectra measured on the (100) face of $[(Me_2N)_3C_3]_2[Pt_2Cl_6]$ at 5 K. Each 0.05 relative absorbance equals ϵ 3.68. t = 244 μ.

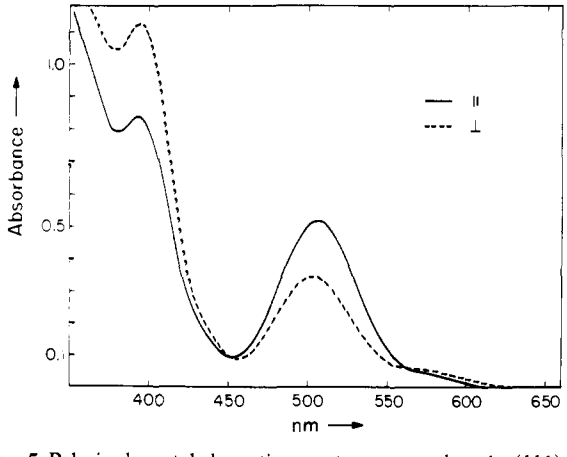

Figure 5. Polarized crystal absorption spectra measured on the (111) face of $[(Me_2N)_3C_3]_2[Pt_2Cl_6]$ at 5 K. Each 0.1 relative absorbance equals ϵ 3.27. t = 137.4 μ.

Cyclopropenium Group. A view of the structure of cation I is shown in Figure 3. The angles and distances found in cations I and II are in good agreement with those observed in other cyclopropenium structures.[21,22] Interestingly, the deviations of the nonhydrogen atoms of each cation from the plane of the cyclopropenium ring correspond in detail with those found in $[(Me_2N)_3C_3][ClO_4]$.[21] For example, in each of the cations in the present structure, two nitrogen atoms are displaced to one side of the ring plane, whereas the remaining nitrogen and all six methyl carbon atoms are displaced to the opposite side.

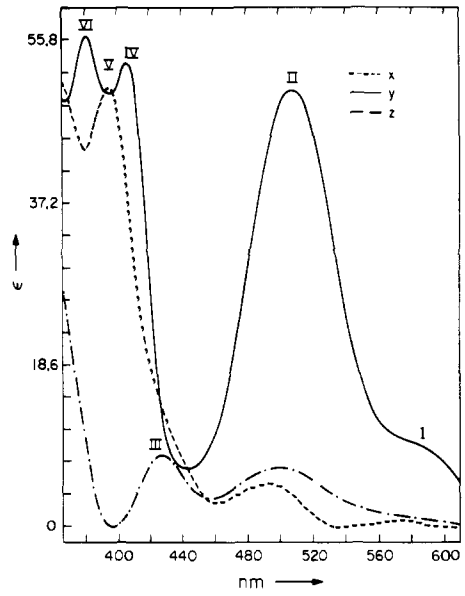

Figure 6. Calculated absorption profiles along the molecular axes of a D_{2h} $Pt_2Cl_6^{2-}$. (X coincides with Pt–Pt; Z is out-of-plane.)

Table VI. Assignments and Polarizations of the Absorption Bands in $Pt_2Cl_6^{2-}$

Band	nm	cm^{-1}	$^1A_g \rightarrow$	Polarization
I	590	16 950	$B_{2u}(^3B_{1u})$	y
II	509	19 650	$B_{2u}(^3A_u)$	y
III	428	23 320	$B_{1u}(^3B_{2u})$	z
IV	407	24 600	$B_{2u}(^1B_{2u})$	y
V	395	25 300	$B_{1g}(^1B_{1g})^a$	x
VI	381	26 250	$B_{2u}(^1B_{2u})$	y

[a] Vibronically allowed.

Electronic Spectra. The liquid helium temperature polarized spectra of the (100) and (111) faces of a single crystal of $[(Me_2N)_3C_3]_2[Pt_2Cl_6]$ are shown in Figures 4 and 5, respectively. The polarized data for the (100) and (111) faces allow resolution of the spectra along the molecular axes (Figure 6).[18] A summary of the spectroscopic data and suggested transition assignments are set out in Table VI.

The positions of bands I through VI are quite similar to well-established features in the polarized electronic spectra of K_2PtCl_4.[4,23-26] Thus, it is likely that bands I, II, and III correspond to spin-forbidden d–d transitions, whereas bands IV, V, and VI are related to the lowest spin-allowed excitation in D_{4h} $PtCl_4^{2-}$, $^1A_{1g} \rightarrow {}^1A_{2g}$ ($d_{x^2-y^2} \rightarrow d_{xy}$). Noteworthy of the features in the polarized spectra of $[(Me_2N)_3C]_2[Pt_2Cl_6]$ that suggest departures from an isolated C_{2v} chromophore model are the intensity and strong y polarization of band II and the appearance of two y-polarized features (IV and VI) in the $^1A_{1g} \rightarrow {}^1A_{2g}$ region.

Interpretation of bands II, IV, and VI may be made under the assumption that metal–metal interactions are not negligible, and that certain d–d transitions acquired allowed character as a result of d electron delocalization over the two Pt centers. In such a situation it is appropriate to analyze the polarizations according to the selection rules of D_{2h} symmetry. It is further assumed that interactions among the D_{2h} chromophores make no contribution to the observed spectra. The allowed d–d transitions predicted for D_{2h} $Pt_2Cl_6^{2-}$ are given in Table VII.

Table VII. Summary of d-d Transitions in D_{2h} $Pt_2Cl_6^{2-}$

Orbital excitations	Transitions[a,b]: $^1A_g \rightarrow$
$d_{x^2-y^2}(\pm) \rightarrow d_{xy}(\pm)$	$2B_{1g}(^1B_{1g})$, $2B_{2u}(^1B_{2u})$
	$2B_{3u}(^3B_{2u})$, $2A_u(^3B_{2u})$, $2B_{1u}(^3B_{2u})$
$d_{xz}(\pm) \rightarrow d_{xy}(\pm)$	$2B_{3g}(^1B_{3g})$, $2A_u(^1A_u)$
	$2B_{1u}(^3A_u)$, $2B_{2u}(^3A_u)$, $2B_{3u}(^3A_u)$
$d_{yz}(\pm) \rightarrow d_{xy}(\pm)$	$2B_{1u}(^1B_{1u})$, $2B_{2g}(^1B_{2g})$
	$2A_u(^3B_{1u})$, $2B_{3u}(^3B_{1u})$, $2B_{2u}(^3B_{1u})$
$d_{z^2}(\pm) \rightarrow d_{xy}(\pm)$	$2B_{1g}(^1B_{1g})$, $2B_{2u}(^1B_{2u})$
	$2B_{3u}(^3B_{2u})$, $2A_u(^3B_{2u})$, $2B_{1u}(^3B_{2u})$

[a] Selection rules are: $^1A_g \rightarrow B_{3u}$, x-allowed; $^1A_g \rightarrow B_{2u}$, y-allowed; $^1A_g \rightarrow B_{1u}$, z-allowed. [b] Spin-orbit coupling is included; excited states derived from gerade triplets are not given.

Bands IV and VI correspond to the two y-allowed transitions, $^1A_g \rightarrow B_{2u}$ ($^1B_{2u}$), derived from $^1A_{1g} \rightarrow {}^1A_{2g}$ ($d_{x^2-y^2} \rightarrow d_{xy}$). The fact that they are split by 1650 cm^{-1} establishes directly that moderate Pt···Pt interactions are present. Overlap between $d_{x^2-y^2}$ orbitals on adjacent Pt atoms could be expected to be fairly substantial, and the resultant Pt···Pt interaction would be repulsive in nature in the ground electronic state of $Pt_2Cl_6^{2-}$. Such a repulsive interaction could be responsible for part of the distortion found in the Pt_2Cl_2 ring (vide supra). The substantial intensity enhancement of band II in the y direction also suggests Pt···Pt interaction. As the d_{xz} orbitals on the two centers should interact relatively more strongly than the d_{yz} ones, the preferred assignment is to the higher energy $^1A_g \rightarrow B_{2u}$ (^3A_u) transition.

The remaining bands in $Pt_2Cl_6^{2-}$ appear to be very closely related to absorptions in $PtCl_4^{2-}$. Band I may be assigned to the $^1A_g \rightarrow B_{2u}$ ($^3B_{1u}$) transition. It is important to note that the virtual absence of x and z absorptions in the region of band I shows conclusively that states derived from $^3A_{2g}$ cannot be lowest in $PtCl_4^{2-}$. The observed polarization behavior of bands I and II of $Pt_2Cl_6^{2-}$, therefore, establishes ^3E_g-derived states to be lowest, and in turn allows the conclusion that ^3E_g is below $^3A_{2g}$ in $PtCl_4^{2-}$. Further, it is likely that the relatively weak x- and z-polarized features at about 20 000 cm^{-1} correspond to $^1A_{1g} \rightarrow {}^3A_{2g}$ in D_{4h} [$^1A_g \rightarrow B_{3u}$, B_{1u} ($^3B_{2u}$) in D_{2h}]. Band III also is observed in x and z polarizations, consistent with its assignment to $^1A_{1g} \rightarrow {}^3B_{1g}$ (D_{4h}) components. Band V is attributed to the vibronically allowed, x-component of $^1A_{1g} \rightarrow {}^1A_{2g}$. Our electronic spectral results for $Pt_2Cl_6^{2-}$ have established, therefore, that the lowest excited states in the $[Pt^{II}Cl_4]$ chromophore increase energetically according to $^3E_g < {}^3A_{2g} < {}^3B_{1g} < {}^1A_{2g}$. Bands III and V are both slightly red shifted (~1 kK) in $Pt_2Cl_6^{2-}$ in comparison to analogous absorptions in $PtCl_4^{2-}$, owing to a small reduction in average ligand field strength associated with the ~0.06 Å elongation of the bridging Pt-Cl bonds.

Acknowledgments. We thank Drs. Richard Eisenberg, D. C. Harris, D. S. Martin, Jr., and Edward Solomon for helpful discussions. This research was supported by the National Science Foundation.

Supplementary Material Available: Structure factor amplitudes (2 pages). Ordering information is given on any current masthead page.

References and Notes

(1) (a) J. S. Miller and A. J. Epstein, *Prog. Inorg. Chem.*, **20**, 1 (1976), and references therein; (b) H. Isci and W. R. Mason, *Inorg. Chem.*, **13**, 1175 (1974), and references therein; (c) D. S. Martin, Jr., R. M. Rush, R. F. Kroening, and P. E. Fenwick, *ibid.*, **12**, 301 (1973), and references therein.
(2) P. Day, M. J. Smith, and R. J. P. Williams, *J. Chem. Soc. A*, 668 (1968).
(3) D. S. Martin, Jr., R. M. Rush, and T. J. Peters, *Inorg. Chem.*, **15**, 699 (1976).
(4) (a) C. J. Ballhausen and H. B. Gray in "Coordination Chemistry", Vol. I, A. E. Martell, Ed., Van Nostrand-Reinhold, New York, N.Y., Chapter 1, and references therein; (b) H. H. Patterson, J. J. Godfrey, and S. M. Khan, *Inorg. Chem.*, **11**, 2872 (1972); (c) R. P. Messmer, L. V. Interrante, and K. H. Johnson, *J. Am. Chem. Soc.*, **96**, 3847 (1974).
(5) J. C. Thibeault, R. F. Ziolo, and H. B. Gray, *Cryst. Struct. Commun.*, **3**, 473 (1974).
(6) D. C. Harris and H. B. Gray, *Inorg. Chem.*, **13**, 2250 (1974).
(7) CRYM is an integrated series of crystallographic routines written by R. E. Marsh and co-workers at the California Institute of Technology (D. J. Duchamp, A.C.A. Meeting, Bozeman, Mont., 1964, paper B-14, p 29).
(8) W. R. Busing and H. A. Levy, *J. Chem. Phys.*, **26**, 563 (1957).
(9) P. Coppens, "Crystallographic Computing", F. R. Ahmed, Ed., Munksgaard, Copenhagen, 1970, p 260.
(10) A. J. C. Wilson, *Nature (London)*, **150**, 152 (1942).
(11) I. L. Karle, K. S. Dragonette, and S. A. Brenner, *Acta Crystallogr.*, **19**, 713 (1965).
(12) E. R. Howells, D. C. Phillips, and D. Rogers, *Acta Crystallogr.*, **3**, 210 (1950).
(13) (a) W. H. Zachariasen, *Acta Crystallogr.*, **16**, 1139 (1963); (b) A. Larson, *ibid.*, **23**, 664 (1967).
(14) H. P. Hanson, F. Herman, J. D. Lea, and S. Skillman, *Acta Crystallogr.*, **17**, 1040 (1964).
(15) D. T. Cromer, *Acta Crystallogr.*, **18**, 17 (1965).
(16) R. F. Stewart, E. R. Davidson, and W. T. Simpson, *J. Chem. Phys.*, **42**, 3175 (1965).
(17) See paragraph at end of paper regarding supplementary material.
(18) C. D. Cowman, Ph.D. Thesis, California Institute of Technology, 1974.
(19) N. C. Stephenson, *Acta Crystallogr.*, **17**, 587 (1964).
(20) K. J. Palmer and N. Elliott, *J. Am. Chem. Soc.*, **60**, 1852 (1938).
(21) A. T. Ku and M. Sundaralingam, *J. Am. Chem. Soc.*, **94**, 1688 (1972).
(22) M. Sundaralingam and L. H. Jensen, *J. Am. Chem. Soc.*, **88**, 198 (1966).
(23) D. S. Martin, Jr., M. A. Tucker, and A. J. Kassman, *Inorg. Chem.*, **4**, 1682 (1965).
(24) O. S. Mortensen, *Acta Chem. Scand.*, **19**, 1500 (1965).
(25) D. S. Martin, Jr., and C. A. Lenhardt, *Inorg. Chem.*, **3**, 1368 (1964).
(26) D. S. Martin, Jr., J. G. Foss, M. E. McCarville, M. A. Rucker, and A. J. Kassman, *Inorg. Chem.*, **5**, 491 (1966).